

Isvector dipole-resonance structure within the effective surface approximation

J P Blocki

National Centre of Nuclear Research, PL-00681 Warsaw, Poland

A G Magner*

Institute for Nuclear Research, Kyiv 03680, Ukraine

P Ring

Technical Munich University, D-85747 Garching, Germany

PACS REF: 21.10.Dr, 21.65.Cd, 21.60.Ev, 24.30.Cz

Abstract

The nuclear isovector-dipole strength structure is analyzed in terms of the main and satellite (pygmy) peaks within the Fermi-liquid droplet model. Such a structure is sensitive to the value of the surface symmetry-energy constant obtained analytically for different Skyrme forces in the leptodermous effective surface approximation. Energies, sum rules and transition densities of the main and satellite peaks for specific Skyrme forces are qualitatively in agreement with the experimental data and other theoretical calculations.

Keywords: *Local density approach, extended Thomas-Fermi model, nuclear symmetry energy, isovector dipole resonances, Fermi-liquid droplet model, strength function, transition density, pygmy resonances.*

1. Introduction

The symmetry energy is a key quantity for studies of the fundamental properties of the exotic nuclei with a large excess of neutrons in the nuclear physics and astrophysics. In spite of a very intensive study of these properties, the surface symmetry energy constant is still rather not well determined in the liquid droplet model (LDM) calculations [1] and in more microscopic local density approach (LDA). In particular, in the extended Thomas-Fermi (ETF) approximation [2], or in models based on the Hartree-Fock (HF) method, both with the Skyrme forces [3, 4, 5], such a situation is rather in contrast to the well known volume symmetry energy constant. The Skyrme force parameters responsible for the surface symmetry energy constant were obtained by comparing the theoretical calculations of the basic static and dynamic characteristics of nuclei with the experimental data. However, besides of difficulties in studying these characteristics away from the nuclear stability line like subtracting curvature and shell effects from the total energy, they are basically insensitive to this constant. Therefore, the experimental [6, 7, 8] and theoretical [9, 10, 11, 12] investigations of the finer structures like the so called [6, 9, 10] pygmy resonances of the

Isvector Dipole Resonance (IVDR) strength become especially interesting as being more sensitive to the value of the surface symmetry-energy constant. Simple and accurate enough analytical theories deriving this constant in terms of the Skyrme force parameters by using the effective surface (ES) approximation are needed [13]. This approximation exploits the property of saturation of the nuclear matter and a narrow diffuse-edge region in finite heavy nuclei. The ES is defined as the location of points of the maximum density gradient. The orthogonal coordinate system related locally to the ES is specified by a distance from a given point to the surface and a tangent coordinate at the ES. In these coordinates, the variational condition of the nuclear energy minimum at the fixed particle and neutron-excess numbers within the LDA is simplified significantly when using the leptodermous expansion over a small parameter $a/R \sim A^{-1/3} \ll 1$ in the LDM [1] or ETF approach [2, 13] (a is of the order of the diffuse edge thickness of the nucleus, R is the mean curvature radius of the ES, and A the number of nucleons in heavy nuclei). The accuracy of the ES approximation in the ETF approach with the spin-orbit (SO) and asymmetry terms was checked by comparing results of the HF and ETF theories for several Skyrme forces [13]. The surface symmetry energy constant is sensitive to the choice of the Skyrme force parameters in the corresponding gradient terms of the symmetry energy density [13].

In the present work, the surface symmetry-energy constant [13] as a function of the Skyrme force parameters is applied to analytical calculations of the energies, energy weighted sum rules (EWSR) and transition densities for the main and its satellite (pygmy) peaks in the IVDR strength function within the Fermi-liquid droplet model (FLDM) [14, 15]. We shall consider the rare (zero sound) quasiparticles'-collision regime (close to the mean field approach), in contrast to the opposite frequent collision (hydrodynamic) regime of the Steinwedel-Jensen (SJ) and Goldhaber-Teller models.

*e-mail: magner@kinr.kiev.ua

2. The Fermi-liquid droplet model

For IVDR calculations, the FLDM based on the linearized Landau-Vlasov equations for the isoscalar $\delta f_+(\mathbf{r}, \mathbf{p}, t)$ and isovector $\delta f_-(\mathbf{r}, \mathbf{p}, t)$ distribution functions can be used in the phase space [14, 15],

$$\frac{\partial \delta f_{\pm}}{\partial t} + \frac{\mathbf{p}}{m_{\pm}^*} \nabla_r [\delta f_{\pm} + \delta(e - e_F)(\delta e_{\pm} + V_{\text{ext}}^{\pm})] = \delta S t_{\pm}. \quad (1)$$

Here $e = p^2/(2m_{\pm}^*)$ is the equilibrium quasiparticle energy ($p = |\mathbf{p}|$) and $e_F = (p_F^{\pm})^2/(2m_{\pm}^*)$ is the Fermi energy. The isotopic dependence of the Fermi momenta $p_F^{\pm} = p_F(1 \mp \Delta)$ is given by a small parameter $\Delta = 2(1 + F'_0)I/3$, where $I = (N - Z)/A$ is the nuclear asymmetry parameter, N and Z are respectively the neutron and proton numbers ($A = N + Z$) [14]. The reason of having Δ is the difference between the neutron and proton potential depths due to the Coulomb interaction. The isotropic isoscalar F_0 and isovector F'_0 Landau interaction constants are related to the incompressibility $K = 6e_F(1 + F_0) \approx 220 - 260$ MeV and the volume symmetry energy $J = 2e_F(1 + F'_0)/3 \approx 30$ MeV constants of the nuclear matter, respectively. The effective masses $m_{\pm}^* = m(1 + F_1/3)$ and $m_{\pm}^* = m(1 + F'_1/3)$ are determined in terms of the nucleon mass m by anisotropic Landau constants F_1 and F'_1 . Equations (1) are coupled by the dynamical variation of the quasiparticles' interaction δe_{\pm} with respect to the equilibrium value $p^2/(2m_{\pm}^*)$. The time-dependent external field $V_{\text{ext}}^{\pm} \propto \exp(-i\omega t)$ is periodic with a frequency ω . For simplicity, the collision term $\delta S t_{\pm}$ is calculated within the relaxation time $\tau(\omega)$ approximation accounting for the retardation effects due to the energy-dependent self-energy beyond the mean field approach [14, 15].

Solutions of equations (1) are related to the dynamic multipole particle-density variations, $\delta \rho_{\pm}(\mathbf{r}, t) \propto Y_{L0}(\hat{r})$, where $Y_{L0}(\hat{r})$ are the spherical harmonics, $\hat{r} = \mathbf{r}/r$. These solutions can be found in terms of the superposition of the plane waves over the angle of a wave vector \mathbf{q} . Their time-dependence is periodic as the external field V_{ext}^{\pm} is also periodic with the same frequency $\omega = p_{\pm}^{\pm} s_{\pm}^{\pm} q/m_{\pm}^*$ where $s^+ = s$, and $s^- = s(NZ/A^2)^{1/2}$. The factor $(NZ/A^2)^{1/2}$ accounts for conserving the position of the mass center for the isovector vibrations. The sound velocities s_n can be found from the dispersion equations [14] as functions of the Landau interaction constants and $\omega\tau$. The ‘‘out-of-phase’’ particle-density vibrations of the s_1 mode involve the ‘‘in-phase’’ s_2 ones inside the nucleus due to the symmetry interaction coupling.

For small isovector and isoscalar multipole ES-radius vibrations of the finite neutron and proton Fermi-liquid drops around the spherical nuclear shape, one has $\delta R_{\pm}(t) = R\alpha_S^{\pm}(t)Y_{L0}(\hat{r})$ with a small time-dependent amplitudes $\alpha_S^{\pm}(t) = \alpha_S^{\pm} \exp(-i\omega t)$. The macroscopic boundary conditions (surface continuity and force-equilibrium

equations) at the ES are given by [13, 14, 15]:

$$u_r^{\pm} \Big|_{r=R} = R\dot{\alpha}_S^{\pm} Y_{L0}(\hat{r}), \quad \delta \Pi_{rr}^{\pm} \Big|_{r=R} = \alpha_S^{\pm} \overline{P}_S^{\pm} Y_{L0}(\hat{r}). \quad (2)$$

The left hand sides of these equations are the radial components of the mean velocity field $\mathbf{u} = \mathbf{j}/m$ and the momentum flux tensor $\delta \Pi_{\nu\mu}$ [14, 15]. Their right hand sides are the ES velocities and capillary pressures. These pressures are proportional to the isoscalar and isovector surface energy constants b_S^{\pm} [13],

$$\overline{P}_S^{\pm} = \frac{2}{3} b_S^{\pm} \rho_{\infty} \mathcal{P}_{\pm} A^{\mp 1/3}, \quad b_S^{\pm} \propto \mathcal{C}_{\pm} \int_0^{\infty} dr \left(\frac{d\rho_{\pm}}{dr} \right)^2, \quad (3)$$

where $\mathcal{P}_+ = (L-1)(L+2)/2$, $\mathcal{P}_- = 1$, $\rho_{\pm} = \rho_n \pm \rho_p$ and $\rho_{\infty} = 3/(4\pi r_0^3) \approx 0.16 \text{ fm}^{-3}$ is the density of the infinite nuclear matter. Coefficients b_S^{\pm} are essentially determined by constants \mathcal{C}_{\pm} of the energy density in front of its gradient density terms $\propto (\nabla \rho_{\pm})^2$. The conservation of the mass center was taken into account in derivations of the second boundary conditions (2) [14, 15]. Therefore, one has a dynamical equilibrium of forces acting at the ES.

3. Response and transition density

The response function, $\chi_{\pm}(\omega)$, is defined as a linear reaction of the average value of a single-particle operator $\hat{F}(\mathbf{r})$ in the Fourier ω -representation to the external field. For convenience, we may consider this field in terms of a similar superposition of the plane waves as for the distribution function δf_{\pm} [14, 15]. In the following, we will consider the long wave-length limit with $\mathcal{V}_{\text{ext}}^{\pm}(\mathbf{r}, t) = \lambda_{\text{ext}}^{\pm, \omega}(t) \hat{F}(\mathbf{r})$ and $\lambda_{\text{ext}}^{\pm, \omega}(t) = \lambda_{\text{ext}}^{\pm, \omega} e^{-i(\omega + i\eta)t}$, where $\lambda_{\text{ext}}^{\pm, \omega}$ is the amplitude and ω is the frequency of the external field ($\eta = +0$). In this limit, the one-body operator $\hat{F}(\mathbf{r})$ becomes the standard multipole operator, $\hat{F}(\mathbf{r}) = r^L Y_{L0}(\hat{r})$ for $L \geq 1$. The response function $\chi_{\pm}(\omega)$ is expressed through the Fourier transform of the transition density $\rho_{\pm}^{\omega}(\mathbf{r})$ as

$$\chi_{\pm}(\omega) = - \int d\mathbf{r} \hat{F}(\mathbf{r}) \rho_{\pm}^{\omega}(\mathbf{r}) / \lambda_{\text{ext}}^{\pm, \omega}. \quad (4)$$

The transition density $\rho_{\pm}^{\omega}(\mathbf{r})$ is obtained through the dynamical part of the particle density $\delta \rho_{\pm}(\mathbf{r}, t)$ in macroscopic models in terms of the solutions $\delta f_{\pm}(\mathbf{r}, \mathbf{p}, t)$ of the Landau-Vlasov equations (1) with the boundary conditions (2) as the same superpositions of plane waves [14]: $\delta \rho_{-}(\mathbf{r}, t) = \rho_{\infty} \alpha_S^{-} \rho_{-}^{\omega}(x) Y_{10}(\hat{r}) e^{-i\omega t}$, where

$$\rho_{-}^{\omega}(x) = \frac{qR}{j'_L(qR)} \left\{ j_1(\kappa) \rho(x) + \frac{d\rho_-}{dx} \frac{g_V}{g_S} \right\}, \quad (5)$$

$$g_V = \int_0^{\bar{\rho}_0} d\rho \sqrt{\rho(1 + \beta\rho)} \kappa^3 j_1(\kappa) / (1 - \rho), \quad (6)$$

$$g_S = \int_0^{\bar{\rho}_0} d\rho \kappa^3 [1 + \mathcal{O}(\bar{\rho}^2)], \quad \kappa = \kappa_o [1 + ax(\rho)/R], \quad (7)$$

$\kappa_o = qR$. The first term in (5) which is proportional to the isoscalar dimensionless density $\rho = \rho_+$ (in units of ρ_∞) accounts for the volume density vibrations. The second term $\propto d\rho_-/dx$ where ρ_- is a dimensionless isovector density ρ_- (in units of $I\rho_\infty$) corresponds to the density variations due to the shift of the ES. The particle number and mass center position are conserved, and $j_n(\kappa)$ and $j'_n(\kappa)$ are the spherical Bessel functions and their derivatives. The upper integration limit $\bar{\rho}_o$ in (6) and (7) is defined as the root of a transcendent equation $x(\rho) + R/a = 0$. We introduced also the dimensionless SO interaction parameter $\beta = \mathcal{D}_+ \rho_\infty / \mathcal{C}_+$ ($\mathcal{D}_+ = -9mW_0/16\hbar^2$, where $W_0 \approx 100 - 130$ MeV·fm⁵ [2, 13]). Several other quantities were also defined by $\tilde{\rho} = (1 - \rho)/c_{\text{sym}}$, $c_{\text{sym}} = a [J/(\rho_\infty |\mathcal{C}_-|)]^{1/2} \approx 2 - 4$, $a = [\mathcal{C}_+ \rho_\infty K / (30 b_{\text{v}}^2)]^{1/2} \approx 0.5 - 0.6$ fm is the diffuseness parameter, $b_{\text{v}} \approx 16$ MeV. Simple approximate expressions for constants b_{S}^\pm can be easily derived in terms of the elementary functions [13]. Note that in these derivations we neglected curvature terms and shell corrections being of the same order. The isovector energy terms were obtained within the ES approximation with high accuracy up to the product of two small quantities, I^2 and $(a/R)^2$. The isovector equilibrium particle density $\rho_-(x)$ in (5) can be given through the isoscalar one, $\rho_+(x) \equiv \rho(x)$. As shown [13], the SO dependent density $\rho_-(x)$ is of the same order as $\rho(x)$. The dependence of the isovector $\rho_-(x)$ on different Skyrme force parameters, mainly \mathcal{C}_- and β , is the main reason of different values of the neutron skin.

With the help of the boundary conditions (2), one can derive the response function (4) [14],

$$\chi_L(\omega) = \sum_n \chi_L^{(n)}(\omega) = \sum_n \mathcal{A}_L^{(n)}(\kappa_o) / D_L^{(n)}(\omega - i\Gamma/2), \quad (8)$$

with $\omega = p_F s_n \kappa_o (NZ/A^2)^{1/2} / (m^* R)$ ($m^*_- \approx m^*_+ = m^*$). This response function describes two modes, the main ($n = 1$) IVDR and its satellite ($n = 2$) as related to the out-of-phase s_1 and in-phase s_2 sound velocities, respectively. We assume here that the “main” peak exhausts mostly the energy weighted sum rule (EWSR) and the “satellite” corresponds to a much smaller value of the EWSR. This two-peak structure is due to the coupling of the isovector and isoscalar density-volume vibrations due to the neutron and proton quasiparticle interaction in (1). The lowest poles ($n = 1, 2$) of the response function (8) are determined by the secular equation,

$$D_L^{(n)} \equiv j'_L(\kappa_o) - \frac{3e_F \kappa_o c_1^{(n)}}{2b_{\text{S}}^- A^{1/3}} \left[j_L(\kappa_o) + c_2^{(n)} j''_L(\kappa_o) \right] = 0. \quad (9)$$

The width of an IVDR peak Γ in (8) as an imaginary part of the pole originated from the integral collision term δSt_\pm of the Landau-Vlasov equation. For amplitudes one has $\mathcal{A}_L^{(n)} \propto \Delta^{n-1}$. The complete expressions for $\mathcal{A}_L^{(n)}$ and $c_i^{(n)}$ are given in [14, 15]. Assuming a smallness of Δ , one may call the $n = 2$ mode as a “satellite” of the “main”

$n = 1$ peak. On the other hand, other factors such as a collisional relaxation time, the surface symmetry energy constant b_{S}^- , and the particle number A lead sometimes to a re-distribution of the EWSR values among these two IVDR peaks. From (9), one can find their splitting [14]:

$$\hbar|\omega^{(1)} - \omega^{(2)}| \approx (10/3)^{3/2} e_F^2 F'_0 I^2 / (|b_{\text{S}}^-| A^{2/3}). \quad (10)$$

This relationship is important for the prediction of distances between the “satellite” and the “main” peaks, depending on the surface symmetry energy constant b_{S}^- , particle number A and interaction constant F'_0 .

According to the time-dependent HF approach based on the Skyrme forces [11, 12], the energy of the pygmy resonances in the isovector and isoscalar channels coincide approximately. On the other hand, the energy of the main peak of the Isoscalar Dipole Resonance (ISDR) is much larger than that of the IVDR. We may try to interpret within the FLDM the satellite peak as some kind of the pygmy one, as observed experimentally, e.g., in some spherical isotopes ²⁰⁸Pb, ¹³²Sn, and ⁶⁸Ni [6, 7]. Therefore, we may calculate separately the neutron, $\rho_n^\omega(x)$, and proton, $\rho_p^\omega(x)$, transition densities for the satellite by calculating the isovector and isoscalar transition densities at the same energy and in the same units as ρ_\pm , $\rho_n^\omega(x) = [\rho_+^\omega(x) \pm \rho_-^\omega(x)] / 2$.

4. Discussion of the results

The total IVDR strength function being the sum of the two (“out-of-phase” $n = 1$ and “in-phase” $n = 2$) strength functions [solid lines in Fig. 1] has rather a remarkable shape asymmetry. In Fig. 1(a) for the SLy5* and (b) SVmas08 cases, one has the “in-phase” satellite on right of the main “out-of-phase” peak. An enhancement on its left for SLy5* is due to the increasing of the “out-of-phase” strength (frequent dashed) curve at too small energies. A more pronounced enhancement is seen for the SVsym32 force in Fig. 1(b) because of the “out-of-phase” satellite (frequent dots), that is in better accordance with the experimental data [6, 7]. This IVDR strength structure is in contrast to the SVmas08 result with the dominating “out-of-phase” peak shown in (b). As seen from comparison in Fig. 1(a) with (b), the shape structure of the total IVDR strength function depends significantly on the surface symmetry energy coefficient $k_{\text{S}}^- = b_{\text{S}}^- / I^2$ where $b_{\text{S}}^- \propto I^2$ [13]. Notice also that one has its strong dependence on the relaxation time τ [see, e.g., curves for the relaxation times τ_1 and τ_2 in Fig. 1(a)]. The “in-phase” strength component with rather a wide maximum is weakly dependent on the choice of the Skyrme forces [3, 4, 5].

Fig. 2 shows the transition particle densities $\rho^\omega(x)$ (5) as functions of the dimensionless radial variable $x = (r - R)/a$ for the isovector vibrations in ¹³²Sn at the same Skyrme forces as in Fig. 1. Results of these calculations look qualitatively similar to those of [9, 11, 12]. The neutron particle density is always significantly larger than the proton one in the surface region $|x| \lesssim 1$. The difference is in a distance

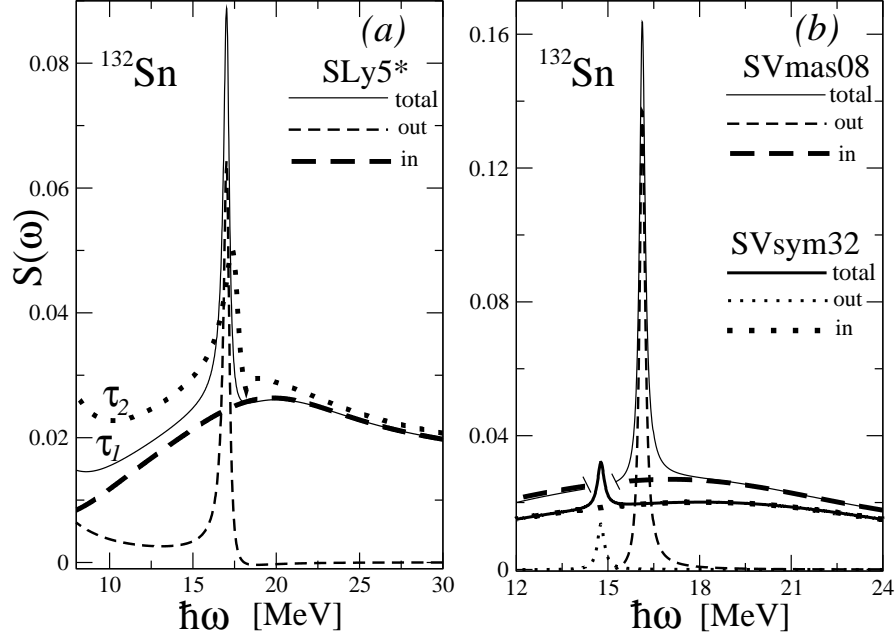


Fig. 1: IVDR strength functions $S^{(n)}(\omega)$ vs the excitation energy $\hbar\omega$ are shown for vibrations of the nucleus ^{132}Sn . (a): The Skyrme force SLy5*; frequent ($n = 1$ “out”), and rare ($n = 2$ “in”) dashed curves and their total sum (solid) are shown; [$\tau_1 = 4.4$ and $\tau_2 = 1.4 \cdot 10^{-21}$ s (dots)]. (b): The same for two other Skyrme forces at the relaxation time with the same frequency dependence as in τ_1 [15];

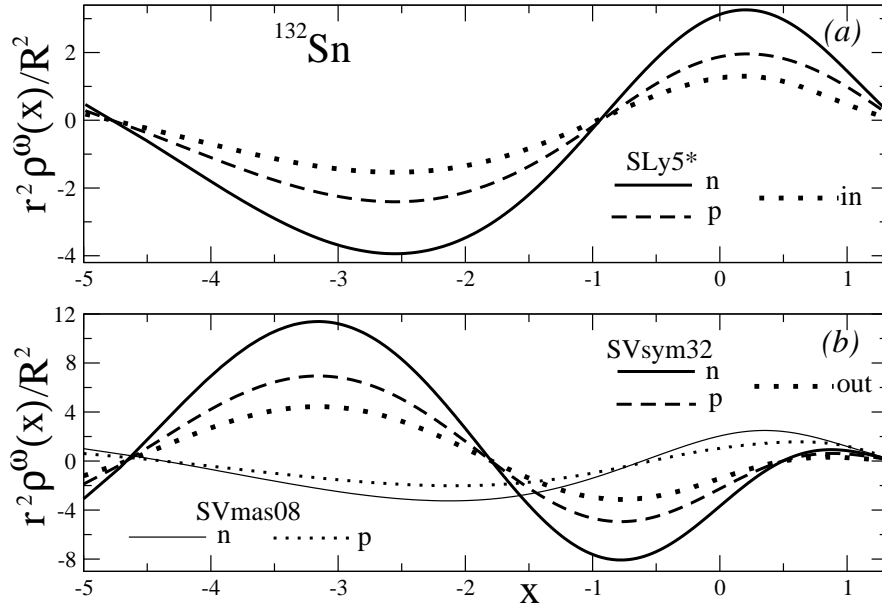


Fig. 2: The IVDR transition densities $\rho_{\pm}^{\omega}(x)$ (5) multiplied by $(r/R)^2$ vs $x = (r - R)/a$ with (a) SLy5* [5] and (b) SVmas08 and SVsym32 [4]; rare dots show the “in-phase” ($n = 2$) mode for SLy5* and “out-of-phase” ($n = 1$) one for SVsym32 at the excitation energies E_2 (Table 1); the neutron ρ_n^{ω} (n) and proton ρ_p^{ω} (p) transition densities for the energy E_2 are shown by the solid and dashed (frequent dots) lines for SLy5* and SVsym32 (SVmas08), respectively.

between the neutron transition density curve and the proton one, but one has always the neutron skin around a symmetric core.

Within the ES approximation, the surface symmetry energy coefficient k_s for three Skyrme forces [4, 5] with a two-peak structure is shown in Table 1. The isovector energy coefficient k_s is more sensitive to the choice of the Skyrme forces than the isoscalar one b_S^+ [13]. The magnitude of k_s for the most of SLy [3], SkI and SV [4] forces is significantly larger than for other ones (the corresponding isovector stiffness Q depending also on the neutron skin [1] was obtained analytically [13]).

According to (3), the most responsible fitting parameters in the Skyrme HF approach which result in significant differences in k_s (or b_S^-) values are the key constants C_- in gradient terms of the energy density, $k_s \propto C_-$ [13]. The constant C_- is strongly dependent on different Skyrme forces (even in sign), in contrast to the isoscalar energy density constants b_S^+ [13]. There are still unclear interpretations of the experimental results [6, 7] which would determine k_s well enough as the mean Isovector Giant Dipole Resonance (IVGDR) energies are almost insensitive to k_s for different Skyrme forces [13]. Another reason for so different k_s values might be related to difficulties in extracting k_s directly from HF calculations due to the curvature and quantum (shell) effects. We have to go also away from the nuclear stability line to extract uniquely the coefficient k_s out of the dependence: $b_S^- \propto I^2 = (N - Z)^2/A^2$. For exotic nuclei, one has more problems to relate k_s to the experimental data with a good enough precision. We emphasize that there is an abnormal behavior of the isovector surface constant k_s as related to the constant C_- of the energy density [13]. This is in contrast to all other Skyrme forces where $k_s < 0$ as $C_- < 0$ with a normal positive isovector stiffness Q of the stable neutron-skin vibrations. For specific Skyrme forces, such as RATP [3], SkI and SV [4], k_s is positive as $C_- > 0$, that could mean one has an abnormal negative isovector stiffness Q of unstable neutron-skin vibrations. For some Skyrme forces like SkT6 [3], the isovector stiffness even diverges, $Q = \infty$, because of $k_s = 0$ ($C_- = 0$). Therefore, it is impossible to excite the isovector neutron-skin vibrations and, as in the hydrodynamic SJ model, we cannot expect pygmy resonances in the IVDR strength.

The FLDM calculations of the IVDR energies E_n and EWSR S_n in terms of the strength distributions $S^{(n)}(\omega) = \text{Im}\chi_1^{(n)}(\omega)/\pi$ [see (8)] at $n = 1$ and $n = 2$ peaks $\omega = \omega_n$ [$S^{(n)} = S^{(n)}(\omega_n)$, Fig. 1] are shown in Table 1. The averaged constants $D = (D_1S^{(1)} + D_2S^{(2)})/[S^{(1)} + S^{(2)}]$ with $D_n = E_n A^{1/3}$ for the neutron-rich spherical (double magic) nuclei ^{208}Pb , ^{132}Sn , and ^{68}Na are shown too. We call the first one the ‘‘main’’ peak defined as it is exhausting mainly the EWSR, $S_n = S^{(n)}E_n/[E_1S^{(1)} + E_2S^{(2)}]$, in contrast to the ‘‘satellite’’ one with a smaller EWSR contribution. The IVDR energies $E_n = \hbar\omega_n = \hbar\kappa_o^{(n)} p_F^- s_n^- / (m^* R)$ were obtained by calculations of the wave numbers $\kappa_o^{(n)}$ as poles ($\kappa_o^{(n)} = q_n R$) of the response

functions $\chi_n(\omega)$ (8) for the sound velocities s_n^- [14, 15]. The $n = 1$ peak coming from the out-of-phase volume vibration of the neutron-vs-proton particle densities with a sound velocity s_1 and the $n = 2$ peak related to the in-phase isoscalar-like sound with a velocity s_2 are excited by the same isovector-like out-of phase vibration of the neutron vs proton Fermi-liquid drop surfaces. Typically, these modes can be assigned respectively as main and satellite peaks because the strength values $S^{(2)}(\omega) \propto \Delta \propto I$ are smaller than $S^{(1)}(\omega)$ of the zero order in I .

A satellite with a relatively smaller EWSR contribution can be interpreted within the FLDM, as a Pygmy Dipole Resonance [9, 11, 12]. These resonances were found for several nuclear isotopes with the Skyrme forces SLy5* [5] or SVmas08 and SVsym34 [4] [see, e.g., Fig. 1(a) or (b) for the nucleus ^{132}Sn]. A smaller contribution at SLy5* and SVmas08 of the in-phase (isoscalar-like volume-compression) density vibrations to the main (out-of-phase) IVDR peak is associated with those discussed in [11, 12] but on its right side. As seen from Fig. 1(b), one has different IVDR strength structures mainly due to the difference in k_s : The in-phase SVsym32 mode becomes even slightly dominating. Note that our FLDM splitting is alternative to the quantum isotopic one which fails for heavy nuclei [14].

5. Summary

Expressions for the surface symmetry energy constant k_s derived from the simple isovector solutions of the particle density and nuclear energy within the leading ES approximation [13] are used in calculations of the energies, sum rules for the IVDR strength and transition densities within the FLDM [14, 15] for some Skyrme forces [4, 5]. The constant k_s depends much on the critical parameters of the Skyrme forces, mainly through C_- of the density gradient terms in the isovector part of the energy density and SO interaction constant β .

IVDR strengths are split into the main and satellite peaks. The mean (IVGDR) energies and EWSR values are in a fairly good agreement with the experimental data. According to our results for the basic IVDR characteristics, the neutron and proton transition densities [Fig. 2], we may interpret semiclassically the IVDR satellites as some kind of the pygmy resonances. Their energies, sum rules and n-p transition densities obtained analytically within the semiclassical FLDM approximation are sensitive to the surface symmetry energy constant k_s . Therefore, their comparison with the experimental data can be used for the evaluation of k_s .

As perspectives, it would be worth to apply our results to the systematic IVDR calculations of the pygmy resonances within the Fermi-liquid droplet model [14, 15] and the isovector low-lying collective states within the periodic orbit theory [16]. They all are expected to be more sensitive to the values of k_s . Our analytical approach without any fitting is helpful for further study of the effects in the

Skymes	^A X	E_1 MeV	S_1 %	E_2 MeV	S_2 %	D_{FLD} MeV	D_{HD} MeV	k_S MeV	Q MeV	C_- MeV·fm ⁵	β	τ ×10 ⁻²¹ s
SLy5*	²⁰⁸ Pb	14.5	74	17.1	26	89	84	-3.94	107	-24.2	-0.58	6.0
	¹³² Sn	17.0	68	19.8	32	91	83					4.4
	⁶⁸ Ni	20.9	61	25.0	39	91	82					2.9
SVmas08	²⁰⁸ Pb	13.9	89	14.8	11	83	101	12.4	-60	36.9	-0.51	7.4
	¹³² Sn	16.1	83	17.1	17	83	104					5.5
	⁶⁸ Ni	20.3	83	21.9	17	84	110					3.5
SVsym32	²⁰⁸ Pb	15.6	53	12.8	47	84	97	3.41	-118	26.0	-0.47	9.9
	¹³² Sn	18.1	64	14.8	36	85	98					7.4
	⁶⁸ Ni	23.4	68	18.7	32	88	101					4.7

Table 1: Energies E_n and EWSR S_n ($S_1 + S_2 = 100$ %) for the out-of-phase $n = 1$ and in-phase $n = 2$ IVDR (or otherwise) are shown for the SLy5* [5] and SVmas08 [4] (but for SVsym32) Skyrme forces; k_S , Q [13], C_- , β and τ [14] at the IVGDR peak are explained in the text; the 7th and 8th columns are the mean (IVGDR) energy constants $D_{FLD}(A)$ averaged with the strength distributions of the desired peaks and $D_{HD}(A)$ [13] calculated within the FLD and HD (SJ) models, respectively.

surface symmetry energy.

Acknowledgement

Authors thank M. Kowal, T. Kozłowski, V.O. Nesterenko, P.-G. Reinhard, and J. Skalski for many useful discussions. One of us (A.G.M.) is also very grateful for a nice hospitality during his working visits at the National Centre of Nuclear Research in Poland. This work was partially supported by the Deutsche Forschungsgemeinschaft Cluster of Excellence Origin and Structure of the Universe (www.universe-cluster.de).

References

- [1] Myers W D, Świątecki W J 1969 Ann. Phys. **55** 395
Myers W D, Świątecki W J 1974 Ann. Phys. **84** 186
- [2] Brack M, Guet C and Hakansson H-B 1985 Phys. Rep. **123** 275
- [3] Chabanat E et al 1997 Nucl. Phys. **A627** 710
Chabanat E et al 1998 Nucl. Phys. **635** 231
- [4] Klüpfel P, Reinhard P-G, Bürvenich T J and Maruhn J A 2009 Phys. Rev. **C79** 034310
- [5] Pastore A et al 2013 Phys. Scr. **T154** 014014
- [6] Adrich P et al 2005 Phys. Rev. Lett., **95** 132501
- [7] Wieland O et al 2009 Phys. Rev. Lett., **102** 092502
- [8] Voinov A et al 2010 Phys. Rev. **C81** 024319
Larsen A C et al 2013 Phys. Rev. **C87** 014319
- [9] Vretenar D, Paar N, Ring P and Lalazissis G A 2001 Phys. Rev. **C63** R13
Vretenar D, Paar N, Ring P and Lalazissis G A 2001 Nucl. Phys. **A692** 496
- [10] Ryezayeva N, Hartmann T, Kalmykov Y et al 2002 Phys. Rev. Lett., **89** 272502
- [11] Repko A, Reinhard R-G, Nesterenko V O and Kvasil J 2013 Phys. Rev. **C87** 024305
- [12] Kvasil J, Repko A, Nesterenko V O, Kleining W, Reinhard R-G 2013 Phys. Scr. **T154** 014019
- [13] Blocki J P, Magner A G, Ring P and Vlasenko A A 2013 Phys. Rev. **C87** 044304

- [14] Kolomietz V M, Magner A G and Shlomo S 2006 Phys. Rev. **C73** 024312
- [15] Magner A G, Gorpinchenko D V and Bartel J 2014 Phys. At. Nucl. in print arXiv:1308.3687 [nucl-th]
- [16] Gzhebinsky A M, Magner A G and Fedotkin S N 2007 Phys. Rev. **C76** 064315